2011 2nd International Conference on Environmental Science and Development
IPCBEE vol.4 (2011) © (2011) IACSIT Press, Singapore

Numerical simulation of a turbidity current flowing over a solid obstacle

Afshin Eghbalzadeh
Department of civil Engineering
Razi University, Assistant Professor
Kermanshah, Iran
e-mail: afeghbal@yahoo.com

Mitra Javan
Department of civil Engineering
Razi University, Assistant Professor
Kermanshah, Iran
e-mail: javanmi@gmail.com

Abstract—**Turbidity currents are often the main process for the transport and deposition of the sediments in narrow dam reservoirs. Turbidity currents with high concentration of suspended sediments follow the thalweg of the lake to the deepest area near the dam, where the sediments can affect the operation of the bottom outlet and the intake structures. The use of solid obstacles is one of the methods for the control of reservoir sedimentation. A two-dimensional (2D) numerical model based on unsteady Reynolds-averaged Navier-Stokes (RANS) equations has been developed for the simulation of turbidity currents driven by non cohesive sediment and flowing over a solid obstacle. The 2D unsteady RANS equations closed by a buoyancy-modified $k-\varepsilon$ turbulence model are integrated in time with a second-order fractional step approach. The results of numerical model have been compared with experimental results. The calculated and measured velocity profiles, front velocities, and sediment depositional depth generally are in good agreement. This demonstrates that the present numerical model can be used for further study on the behavior of turbidity currents that encounter solid obstacles.**

Keywords-component; numerical simulation; turbidity currents; turbulence; dam reservoir

I. INTRODUCTION

Today's worldwide annual mean loss of storage capacity due to sedimentation is already higher than the increase of capacity by construction of new reservoirs for irrigation, water supply, and hydropower. Turbidity currents are sediment-laden underflows that are driven by a density difference with the ambient fluid. They often occur in the oceans, lakes and reservoirs, and constitute an important mechanism for the transport of littoral sediment to deeper waters [1]. In narrow reservoirs with rather steep bottom slopes, turbidity currents are often the main process for the transport and deposit of sediments [2]. These turbidity currents with high sediment concentrations mainly occur during floods and follow the thalweg to the deepest zones of the reservoir near the dam, where the sediments settle down and cover the bottom outlet, or interfere with the operation of the intake structures [3].

The measured velocities of the turbidity currents along the lake bottom can reach high velocities up to 0.5–0.8 m/s during floods [4]. Previously deposited particles can be eroded again and transported further downstream toward the dam. The resulting introduction of additional suspended sediments into a turbidity current increases its density and consequently its velocity [1]. On the other hand, turbidity currents slow down on low slopes, which causes the sediments to settle and the current to die out [5].

If turbidity currents can be entirely stopped in a reservoir, or influenced in such a way that the sediments are not deposited at critical locations including in front of intakes and bottom outlets, the sustainability of reservoir operation is considerably increased. This can be done by a solid obstacle placed in the reservoirs [3].

Several laboratory experiments [6-8] and numerical studies of turbidity currents and their deposits have been carried out during the past several decades. Unsteady numerical simulations of turbidity currents were mostly of depth-averaged type, single-layer formulations based on the finite volume or finite-element methods [9-11]. Reference [11]'s model was also capable of tracking the evolution and development of an erodible bed due to sediment entrainment and deposition. Depth-averaged models obscure the vertical structure of turbidity currents which is of fundamental importance due to the fact that these currents are highly stratified.

Some authors have considered the problem by solving the whole set of the three-dimensional (3D) Navier–Stokes equations using some kind of turbulence model to close the system. Olsen and Tesaker compared numerical simulations of a turbidity current flowing down a slope with physical measurements [12].

3D numerical simulation is computationally expensive. Solution of the Reynolds-averaged Navier-Stokes (RANS) equations with two-dimensional (2D) vertical model is an attractive option. Choi and Garcia simulated two-dimensional saline density currents developing on a slope with the $k-\varepsilon$ turbulence model [13]. Huang et al. studied turbidity currents on an arbitrary slope by solving the unsteady RANS equation with buoyancy modified $k-\varepsilon$ turbulence closure [14-15].

The effects of obstacles on density currents have mainly been investigated by making use of the shallow water analysis [16-18]. Numerical simulations and physical experiments for a turbidity current flowing over a solid obstacle were carried out by Oehy and Schleiss [3]. The investigated measures were also simulated by means of a two-dimensional numerical model, based on the flow solver CFX-4.4.

Existing commercial codes have some limitations. For instance, the memory requirements and execution time are often excessive for solving hydraulic engineering problems.

The CFD software is also very expensive. It is beneficial to develop and validate a new numerical model that can speedily solve the specific problems in hydraulic engineering.

In this paper we develop and apply a robust and second-order-accurate 2D numerical model to simulate the turbidity currents around solid obstacles. The model developed simulates the spatial and temporal evolution of a turbidity current that is allowed to freely exchange sediment with the bottom boundary. The model employs the Boussinesq form of the unsteady RANS equations in conjunction with a buoyancy-extended $k-\varepsilon$ closure for the turbulence [19]. The 2D unsteady RANS equations are integrated in time with a second-order fractional step approach. A second-order accurate semi-Lagrangian technique is used for discretizing the convective terms. We compare the results with the experimental measurements published in [3].

II. Governing Equations

In this study we focus on flows with relatively small density differences for which the usual Boussinesq approximation can be assumed to be valid—i.e. all variations in density can be neglected except for the buoyancy term. Incorporating the Boussinesq hypothesis to relate the Reynolds stresses with the mean rate of strain tensor via an eddy viscosity, 2D unsteady RANS equations for incompressible, stratified flow read as:

$$\frac{\partial u_i}{\partial x_i}=0 \tag{1}$$

$$\frac{\partial u_i}{\partial t}+\frac{\partial u_i u_j}{\partial x_i}=-\frac{(\rho-\rho_\circ)}{\rho_\circ}g_i-\frac{1}{\rho_\circ}\frac{\partial P^*}{\partial x_i}+\frac{\partial}{\partial x_j}\left((\nu+\nu_t)(\frac{\partial u_i}{\partial x_j}+\frac{\partial u_j}{\partial x_i})\right) \tag{2}$$

where u_i and u_j are the Reynolds-averaged velocity components in x and z directions, respectively; $\rho_\circ$ is the density of the ambient fluid; g_i is the acceleration due to gravity; ν and ν_t are the molecular and eddy viscosity, respectively; ρ is the local mixture density and t is time. $P^*=P-\rho_\circ gh$ is the modified pressure including the gravity terms where P is total pressure and h is distance from the reference in z direction.

The eddy viscosity is modeled by the buoyancy-modified $k-\varepsilon$ turbulence model as [19]:

$$\nu_t=C_\mu\frac{k^2}{\varepsilon} \tag{3}$$

where k is the turbulent kinetic energy, ε is its dissipation rate, and C_μ is a model constant. Quantities of k and ε are obtained from the solution of the transport equations:

$$\frac{\partial k}{\partial t}+\frac{\partial u_i k}{\partial x_i}=\frac{\partial}{\partial x_i}\left((\nu+\frac{\nu_t}{\sigma_k})\frac{\partial k}{\partial x_i}\right)+P_r+B-\varepsilon \tag{4}$$

$$\frac{\partial \varepsilon}{\partial t}+\frac{\partial u_i \varepsilon}{\partial x_i}=\frac{\partial}{\partial x_i}\left((\nu+\frac{\nu_t}{\sigma_\varepsilon})\frac{\partial \varepsilon}{\partial x_i}\right)+C_{1\varepsilon}\frac{\varepsilon}{k}(P_r+C_{3\varepsilon}B)-C_{2\varepsilon}\frac{\varepsilon^2}{k} \tag{5}$$

In the above equations, P_r and B are production terms of turbulent kinetic energy due to the mean velocity gradient and the buoyancy. σ_k, σ_ε are turbulent Prandtl number for k and ε, respectively. $C_{1\varepsilon}$, $C_{2\varepsilon}$ and $C_{3\varepsilon}$ are turbulence model constants. The following standard values are specified for the turbulence model constants [20]:

$$C_\mu=0.09,\ C_{1\varepsilon}=1.44,\ C_{2\varepsilon}=1.92,\ \sigma_k=1.0,\ \sigma_\varepsilon=1.3 \tag{6}$$

The range $C_{3\varepsilon}=0-0.4$ has been reported to give a good match with experimental results on density currents [21]. An alternative approach to selecting a constant value is to employ the relation of $C_{3\varepsilon}=\tanh|w/u|$ base on local mean velocity components for mixed flows [22], which has been accepted by several researchers [14-15, 23]. We had carried out numerical simulations using the relation of [22].

The unsteady RANS and turbulence closure equations are solved simultaneously with the following transport equation for the concentration of sediments c, which is used to determine scalar transport and the variation of the fluid density:

$$\frac{\partial c}{\partial t}+\frac{\partial\left((u_j-w_s\delta_{j2})c\right)}{\partial x_j}=\frac{\partial}{\partial x_j}\left((\nu+\frac{\nu_t}{\sigma_t})\frac{\partial c}{\partial x_j}\right) \tag{7}$$

where c is the Reynolds-averaged volumetric concentration of sediments; σ_t is the turbulent Prandtl number for the source of gravity current (in this study, concentration of sediments c); w_s is the sediment fall velocity; and δ_{j2} is Kronecker delta; with coordinate j index 2 indicating the opposite direction of gravity.

Density is assumed to be linearly related to the mean volumetric concentration through the equation of state as $\rho=\rho_\circ+c(\rho_s-\rho_\circ)$ where ρ_s is density of the sediment grains.

III. Boundary Conditions

The boundaries of the computational domain are inlet, outlet, free-surface and solid walls. Flat, slip boundary

condition of zero velocity gradient normal to the surface is applied and the pressure is set equal to the atmospheric value at the surface. The dissipation rate ε is calculated from the relation given by Rodi [19]:

$$\varepsilon = k^{3/2}/(0.43D) \qquad at \quad z = z_s \tag{8}$$

where D is the local water depth and z_s is the coordinate of free surface.

The wall function approach is used to specify boundary conditions at the bottom of the channel in order to avoid the resolution of viscous sublayer [24]. The first grid point off the wall (center of the control volume adjacent to the wall) is placed inside the logarithmic layer ($z_2^+ = u_* z_2'/\nu > 11.6$). The near-wall values of turbulent kinetic energy k and dissipation rate ε are given as:

$$k = u_*^2/C_\mu^{1/2} \qquad \text{and} \qquad \varepsilon = u_*^3/(\kappa z_2') \tag{9}$$

where z_2' is the normal distance to the wall; $u_* = \sqrt{\tau_w/\rho}$ is the bed shear velocity; κ is von Karman constant (=0.41)

On the other hand, if the first grid node from the wall locates within the viscous layer $(z_2^+ < 11.6)$, these near-wall values are approximated as [25]:

$$k = \frac{(z_2')^2 {u_*}^4}{(11.6\nu)^2 c_\mu^{1/2}} \quad and \quad \varepsilon = \frac{2\nu k}{(z_2')^2} \tag{10}$$

Known quantities are specified at the inlet for the inflow velocity, the concentration of the gravity current source, the current thickness, turbulent kinetic energy and dissipation rate. At the outlet the normal gradients of all dependent variables are set equal to zero.

The bed level variation at every time increment *dt* is calculated as:

$$\Delta z_{bed} = \frac{(D-E)dt}{(1-\lambda)} \tag{11}$$

where D and E are the sediment deposition and entrainment rates, respectively and λ is the porosity of the bed sediment. The sediment deposition rate D is calculated as in [1,4,26].

Sediment entrainment to the water column was estimated using the established empirical formula derived by Smith and Maclean [27].

IV. Numerical Method

In this section we present a brief overview of the numerical approach we employ to carry out our simulations. A fractional step method is employed to integrate the 2D governing equations in time coupled with a projection method for satisfying the continuity equation [29,30]. Following [29], dimensional splitting is used to reduce the solution of the 2D problem to a sequence of one-dimensional problems. Non-uniform bathymetry of the computational domains is handled by the sigma-type body-fitted grids which fit the vertical direction of the physical domain [31]. The fractional step approach for solving the momentum equations is also employed to integrate the transport equations for the turbulence quantities and the concentration of sediments. For the later equations only the advection and diffusion steps are required. For the former equations, however, the diffusion step is followed by a step in which the source terms are taken into account explicitly.

We employ the semi-Lagrangian method based on the Fromm scheme for discretization of the advection terms [32]. The spatial derivatives in the diffusion and the projection steps are discretized by finite-volume integration method using the Gauss divergence theorem in terms of the one-order-lower derivatives at the edges of the respective control volume.

The pressure-Poisson equation is solved using a block tri-diagonal algorithm. After calculating the velocity components and pressure field in new time step, the transport equations for the turbulence kinetic energy, energy dissipation rate and sediment concentration are solved using the same fractional step algorithm used to integrate the momentum equations. Finally the density is calculated using the state equation. If the bed elevation changes due to sediment entrainment or deposition, the grid is reorganized by uniformly distributing bed level change Δz_{bed} to all the grid points above it except the one at the free surface.

V. Results

We report simulation results of a turbidity current flowing over a solid obstacle on a flat bed. The simulation case is one of a series of experiments carried out by Oehy and Schleiss [3]. The experiments were carried out in a flume with a length of 8.55 m and width of 0.27 m and a depth of 0.9 m. A sluice gate allowed the release of the turbidity current in the downstream part simulating a reservoir.

The current thickness at the inlet was set equal to 4.5 cm with the help of a sluice gate and the inflow rate per unit width was set equal to 26.1 cm^2/s, which gave a layer-averaged inlet velocity of 5.8 cm/s. For the experiment a cohesionless, fine ground polymer with a density of $\rho_s = 1135\ kg/m^3$ and a particle diameter of $d_{50} = 90\ \mu m$ ($d_{16} = 16\ \mu m$, $d_{84} = 130\ \mu m$) was chosen. The material had a Stokes' settling velocity of 0.45 mm/s and a fairly narrow grain size distribution $\sigma_g = \sqrt{d_{84}/d_{16}}\, d_{50} = 1.6$, slightly skewed toward large grain sizes.

The solid obstacle used in this study was a ridge of 24 cm height, extending across the full width of the flume at a distance of $x_m = 5\ m$ from its inlet. It had a Gaussian shape defined by:

$$z = 0.24\, e^{-50(x-x_m)^2} \qquad (12)$$

where z is the coordinate perpendicular to the bottom; x is the longitudinal coordinate along the flume; h_m is the maximum height of the obstacle and x_m is the position of the maximum height in meters.

Numerical simulation are carried out for one of the experimental configurations [3], which involved a turbidity flow with excess fractional density equal to 0.00329. An 8 m long computational domain is employed in order to avoid reflections from the outlet. A uniform mesh consisting of 425×80 control volumes is used for the simulation. The time step is equal to 0.05 sec.

The calculated sediment concentrations are shown in Fig. 1 by isolines. The sequence with a time interval of 20 s starts just before the turbidity current encounters the obstacle. When the turbidity current reaches the obstacle, it climbs up, decelerating only slightly (see Fig. 1). The turbidity current head then passes over the obstacle. The normal shape of the frontal region is reestablished at some distance downstream of the obstacle. Due to the presence of the obstacle, the flow rate is changed and an internal bore travels upstream.

Computed profiles of streamwise velocity are compared with the values determined from measurements in the quasi-steady part of the turbidity current body. The computed and measured velocity profiles are plotted in Fig. 2 at locations upstream ($x = 3.2\ m$) and downstream ($x = 6.2\ m$) of the solid obstacle. It can be seen that the numerical results agree fairly well with the measured distribution of the streamwise velocity. Due to the effect of the obstacle, the downstream velocity is strongly reduced, whereas the height increased.

Simulated depositional depths as a function of distance from the inlet are plotted in Fig. 3 against experimental data. This period of time corresponds to 520 s. The agreement between the simulation and measured values is obvious. But near the obstacle, the deposition rate is underestimated by the numerical model.

VI. Conclusions

In order to ensure the sustainable use of man-made reservoirs the management of sedimentation is a challenge for designers and dam operators. Turbidity currents can be considerably slowed down by obstacles and that most of the sediments can be retained on their upstream side. A numerical model for a turbidity current flowing over a solid obstacle has been developed. The model is based on the unsteady RANS equations and uses a buoyancy-modified $k-\varepsilon$ closure for the turbulence. The model simulation results have been compared with the experimental data of Oehy and Schleiss [3]. The calculated and measured velocity profiles, front velocities, and sediment depositional depth generally are in good agreement. Therefore, the proposed numerical model is a useful tool for sensitivity analyses of the various parameters such as obstacle height and form, as well as location within a reservoir.

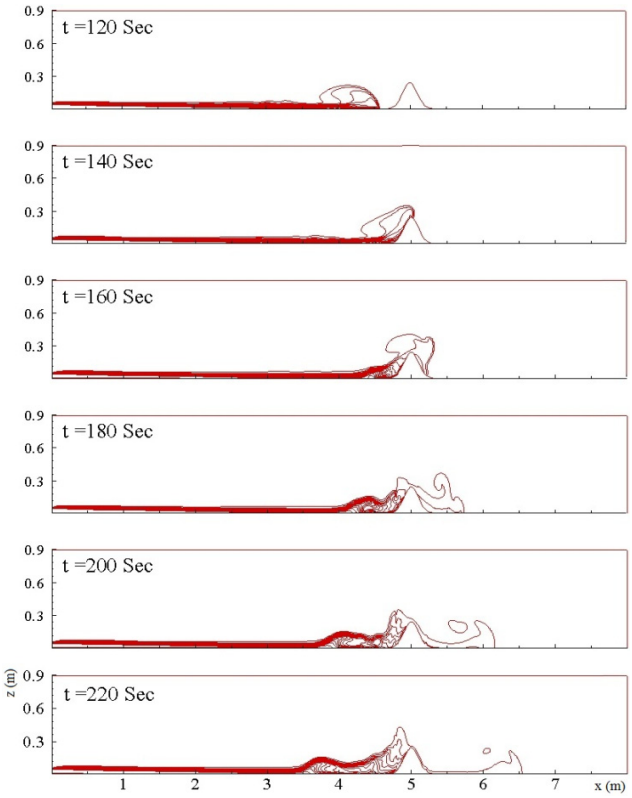

Figure 1. Numerical simulation of turbidity current influenced by obstacle for time steps of 20 s. Lines of equivalent concentration are shown with intervals of 0.1 g/L.

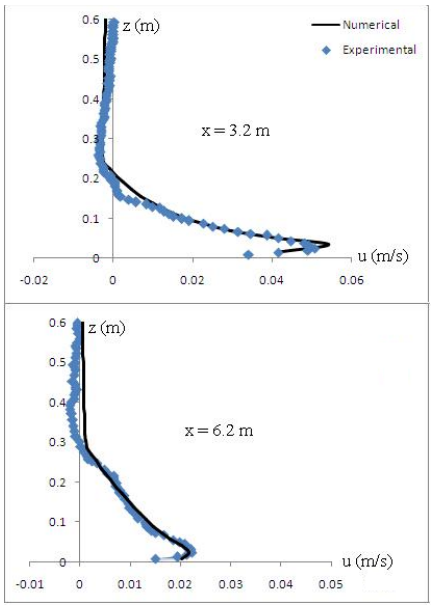

Figure 2. Vertical velocity profiles upstream and downstream of obstacle

References

[1] G. Parker, Y. Fukushima and H. M. Pantin, "Self-accelerating turbidity currents," J. of Fluid Mechanics, vol. 171, 1986, pp. 145–181, doi: 10.1017/S0022112086001404

[2] J. Fan and G. L. Morris, "Reservoir sedimentation I: delta and density current deposits," J. of Hydraulic Engineering, vol. 118, no. 3, 1992, pp. 354–369, doi: 10.1061/(ASCE)0733-9429(1992)118:3(354)

[3] C. Oehy and A. J. Schleiss, "Control of turbidity currents in reservoirs by solid and permeable obstacles," J. of Hydraulic Engineering, vol. 133, no. 6, 2007, pp. 637–648, doi: 10.1061/(ASCE)0733-9429(2007)133:6(637)

[4] G. De Cesare, A. Schleiss and F. Hermann, "Impact of turbidity currents on reservoir sedimentation," J. of Hydraulic Engineering, vol. 127, no. 1, 2001, pp. 6–16, doi: 10.1061/(ASCE)0733-9429(2001)127:1(6)

[5] M. S. Altinakar, W. H. Graf and E. J. Hopfinger, "Weakly depositing turbidity current on a small slope," J. of Hydraulic Research, vol. 28, no. 1, 1990, pp. 55–80, doi: 10.1080/00221689009499147

[6] G. Parker, M. H. Garcia, Y. Fukushima and W. Yu, "Experiments on turbidity currents over an erodible bed," J. of Hydraulic Research, vol. 25, no. 1, 1987, pp. 123–147, doi: 10.1080/00221688709499292

[7] M. H. Garcia and G. Parker, "Experiments on the entrainment of sediment into suspension by a dense bottom current," J. of Geophysical Research [Oceans], vol. 98, issue. C3, 1993, pp. 4793–4807, doi: 10.1029/92JC02404

[8] M. Altinakar, W. Graf and E. Hopfinger, "Flow structure of turbidity currents," J. of Hydraulic Research, vol. 34, no. 5, 1996, pp. 713–718,

[9] G. Parker, "Conditions for the ignition of catastrophically erosive turbidity currents," Marine Geology, vol. 46, 1982, pp. 307–327, doi: 10.1016/0025-3227(82)90086-X

[10] S. U. Choi, "Layer-averaged modeling of two-dimensional turbidity currents with a dissipative-Galerkin finite-element method— Part II: Sensitivity analysis and experimental verification," J. of Hydraulic Research, vol. 33, no. 5, 1999, pp. 623–648, doi: 10.1080/00221689909498310

[11] S. F. Bradford and N. D. Katopodes, "Hydrodynamics of turbid underflows. I: Formulation and numerical analysis," J. of Hydraulic Engineering, vol. 125, no. 10, 1999, pp. 1006–1015, doi: 10.1061/(ASCE)0733-9429(1999)125:10(1006)

[12] N. R. B. Olsen, and E. Tesaker, "Numerical and physical modeling of a turbidity current," Proc. 26th IAHR Biennial Congress. HYDRA 2000, London, 1995, pp. 57-64,

[13] S. Choi and M. H. García, "$k-\varepsilon$ turbulence modeling of density currents developing two dimensionally on a slope," J. of Hydraulic Engineering, vol. 128, no. 1, 2002, pp. 55–63, doi: 10.1061/(ASCE)0733-9429(2002)128:1(55)

[14] H. Huang, J. Imran and C. Pirmez, "Numerical model of turbidity currents with a deforming bottom boundary," J. of Hydraulic Engineering, vol. 131, no. 4, 2005, pp. 283–293, doi: 10.1061/(ASCE)0733-9429(2005)131:4(283)

[15] H. Huang, J. Imran and C. Pirmez, "Numerical modeling of poorly sorted depositional turbidity currents," J. of Geophysical Research, vol. 112, C01014, 2007, pp. 1–15, doi: 10.1029/2006JC003778

[16] J. W. Rottman, J. E. Simpson, J. C. R. Hunt and R. E. Britter, "Unsteady gravity current flows over obstacle: Some observations and analysis related to phase II trials," J. of Hazard Materials, vol. 11, pp. 325–340,

[17] G. F. Lane-Serff, L. M. Beal and T. D. Hadfield, "Gravity current flow over obstacles," J. of Fluid Mechanics, vol. 292, 1995, pp. 39–53, doi: 10.1017/S002211209500142X

[18] P. G. Baines, Topographic effects in stratified flows. Cambridge University Press, U.K.: Cambridge, 1995.

[19] W. Rodi, Turbulence models and their applications in hydraulics-a state-of-arts review. IAHR Monograph, Balkema, Rotterdam, The Netherlands, 1993.

[20] W. Rodi, "Examples of calculation methods for flow and mixing in stratified fluids," J. of Geophysical Research [Oceans], vol. 92, no. C5, 1987, pp. 5305–5328, doi: 10.1029/JC092iC05p05305

[21] Y. Fukushima and N. Hayakawa, "Analysis of inclined wall plume by the $k-\varepsilon$ turbulence model," J. of Applied Mechanics, vol. 57, issue. 2, 1990, pp. 455–465, doi: 10.1115/1.2892011

[22] R. A. W. M. Henkes, F. F. Van Der Vlugt and C. J. Hoogendoorn, "Natural convection flow in a square cavity calculated with low-Reynolds number turbulence models," Int J. of Heat and Mass Transfer, vol. 34, issue. 2, 1991, pp. 377-388, doi: 10.1016/0017-9310(91)90258-G

[23] J. Imran, A. Kassem and S. M. Khan "Three-dimensional modeling of density current. I. Flow in straight confined and unconfined channels," J. of Hydraulic Research, vol. 42, no. 6, 2004, pp. 578–590, doi: 10.1080/00221686.2004.9628312

[24] W. Wu, W. Rodi and T. Wenka, "3D numerical modeling of flow and sediment transport in open channels," J. of Hydraulic Engineering, vol. 126, no. 1, 2000, pp. 4–15, doi: 10.1061/(ASCE)0733-9429(2000)126:1(4)

[25] P. A. Durbin and B. A. Pettersson Reif, Statistical theory and modeling for turbulent flows. Wiley, 2001.

[26] E. W.. Dietrich, "Setting velocity of natural particles," J. of Hydraulic Engineering, vol. 18, no. 6, 1982, pp. 1615-1626, doi: 10.1029/WR018i006p01615

[27] J. D. Smith and S. R. Mclean, "Spatially averaged flow over a wavy surface," J. of Geophysical Research [Oceans], vol. 82, no. 12, 1977, pp. 1735-1746, doi: 10.1029/JC082i012p01735

[28] W. R. Brownlie, "Prediction of flow depth and sediment discharge in open channels," Reprt No. KH-R-43A, Keck Laboratory of Hydraulics and water Resourse California Institute of technology, 1981,

[29] N. N. Yanenko, The Method of Fractional Steps. Springer-Verlag, Berlin, 1971.

[30] A. Eghbalzadeh, M. M. Namin, S. A. A. Salehi, B. Firoozabadi and M. Javan, "URANS simulation of 2D continuous and discontinuous gravity currents," J. of Applied Sciences, vol. 8, no. 16, 2008, pp. 2801-2813.

[31] M. M. Namin, B. Lin and R. A. Falconer, "An implicit numerical algorithm for solving non-hydrostatic free-surface flow problems," Int. J. for Numerical Methods in Fluids, vol. 35, 2001, pp. 341–356, doi: 10.1002/1097-0363(20010215)35:3<341::AID-FLD96>3.0.CO;2-R

[32] J. E. Fromm, "A method of reducing dispersion in convective difference schemes," J. of Computational Physics, vol. 3, issue 2, 1968, pp. 176–189, doi: 10.1016/0021-9991(68)90015-6

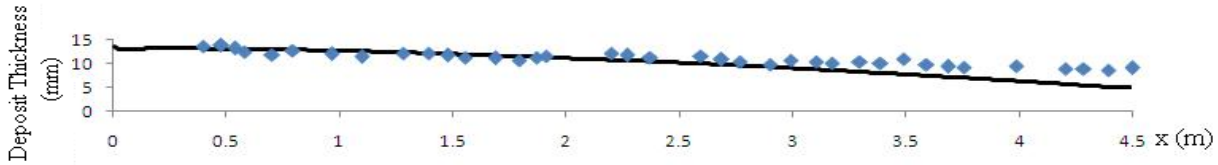

Figure 3. Measured (points) and computed (solid line) deposit thickness upstream of the obstacl